

Research Article

Comparison of Cavity Receivers with and without Mouth-Blockage of Different Shapes and Sizes Used in Paraboloid Dish Applications*

R. D. Jilte, S. B. Kedare, and J. K. Nayak

Department of Energy Science and Engineering, IIT Bombay, Mumbai, MH 400076, India
Address correspondence to J. K. Nayak, jknayak@iitb.ac.in

Received 26 February 2012; Accepted 6 March 2012

Abstract Numerical three-dimensional studies of the natural convection and radiative heat loss from cavity receiver of different shapes with and without mouth-blockage have been investigated under isothermal wall condition. Convective heat loss is found to decrease for cavities having mouth blockage created by reducing aperture area (case I) whereas it enhances when mouth blockages are introduced by increasing the cavity dimensions and keeping the same aperture area (case II). Convective loss is characterized by using the convective zone area (A_{cb}'). Conical cavity yields the lowest convective loss whereas hetro-conical cavity gives the highest convective loss among different shapes investigated. Radiative loss is independent of cavity inclination and is found to be nearly constant for all cavity shapes and cavity configurations (with or without mouth blockage) so long as the aperture area remains the same; it is proportional to the aperture area. However, investigations on decrease in heat loss of mouth-blocked cavities needed to be coupled with the estimation of concentrated flux.

Keywords parabolic dish-receiver systems; open cavity; natural convection heat loss

1 Introduction

The paraboloid dish-receiver assembly is used for applications of solar energy at higher temperature. The receiver is placed at the focus of the paraboloid dish. Generally, a cavity receiver is used to capture the flux at focus and has low heat loss (Harris and Lenz [2]). The heat loss includes convective and radiative losses through the opening of the cavity and conductive losses through the insulation used behind the cavity surfaces.

The literature reports investigations on various types of solar cavities. The present study focuses on the cavities meant for paraboloid dish concentrator and compares

heat loss of cavities with and without mouth-blockages. Different cavity shapes with mouth-blockage are reported: spherical (Leibfried and Ortjohann [4]), cylindrical with conical frustum (McDonald [5]), cylindrical (Taumoefolau et al. [7]) and hemispherical with aperture plate (Reddy and Sendhilkumar [6]). In all these investigations, convective loss is reported to be reducing with the decrease of aperture area. These studies were conducted under different geometrical and operating conditions. Hence, the results cannot be compared and cavity with minimum heat loss cannot be identified. The objective of the present work is to study heat loss from cavities with different shapes, sizes, and configuration (with and without mouth blockage) on a common basis. This will also help in determining the cavity shape with minimum heat loss.

2 Types of cavities investigated

The common terms used for cavity receiver is shown in Figure 1. The philosophy used for comparing open cavities is as follows. For a given paraboloid dish-receiver system with predefined optics, the concentration ratio and focus diameter are fixed and aperture area of the cavity receiver which receives reflected solar radiation from dish has to match the focus diameter. Hence if mouth blockage is introduced, then the receiver will receive reduced flux. Alternatively to avoid this situation, the cavity

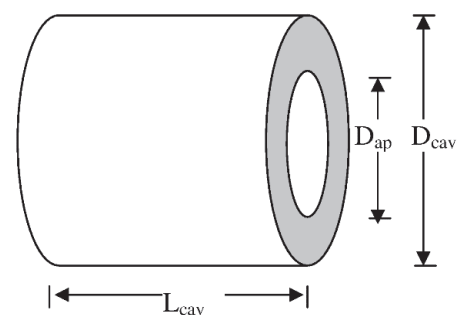
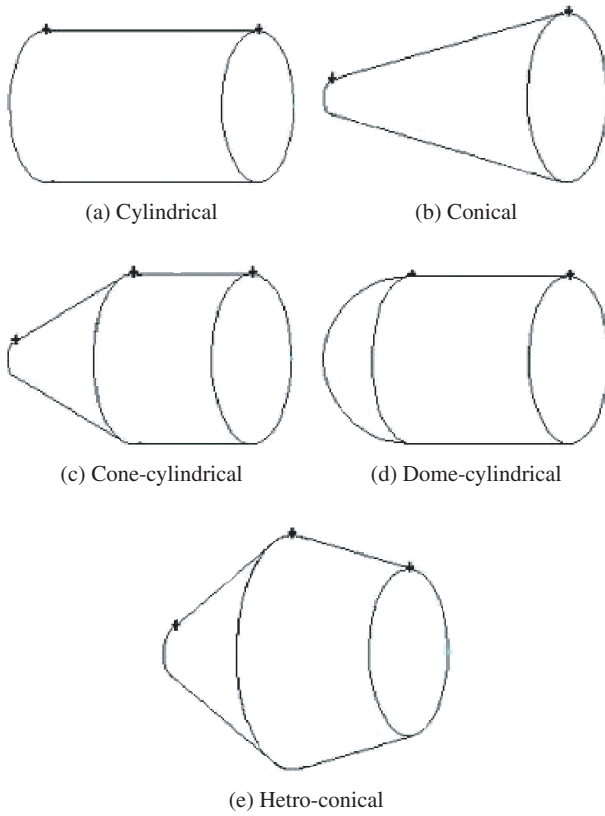


Figure 1: Geometrical parameters used for open cavity.

*This article is a part of a Special Issue on the International Conference on Energy Security, Global Warming and Sustainable Climate (SOLARIS 2012).

Table 1: Geometrical details of the cavities investigated.

	Internal surface area of cavity (m ²)				
	Cylindrical	Conical	Cone-cylindrical	Dome-cylindrical	Hetro-conical
With-blockage case I D _{ap} = 0.4 m, D _{cav} = 0.5 m, L _{cav} = 0.75 m	1.444	0.8	1.06	1.248	1.444
With-blockage case II D _{ap} = 0.5 m, D _{cav} = 0.625 m, L _{cav} = 0.9375 m	2.258	1.265	1.59	1.951	2.223
No-blockage, Case III D _{ap} = D _{cav} = 0.5 m, L _{cav} = 0.75 m	1.374	0.739	0.989	1.178	1.374

**Figure 2:** Shapes of the cavities investigated.

diameter is increased such that the aperture with mouth blockage matches the focus size. Mouth-blocked cavities are created either by reducing aperture diameter (in the form of providing an additional circular ring (case I)) or by increasing cavity dimensions and keeping the same aperture diameter (case II). Cavities without-mouth blockages are referred to as case III. For case III type of cavities, the aperture diameter and cavity diameter are taken as equal to 0.5 m and depth of the cavity as 0.75 m. In case I type of cavities, the aperture diameter is reduced by 20% with the same depth of the cavity whereas in case II type of cavities, cavity dimensions are increased by a factor of 1.25, keeping the same aperture diameter as case III. The geometrical dimensions used in the present study are given in Table 1.

The cavity shapes investigated in the present work are as follows: cylindrical, conical, cone-cylindrical (combination of frustum of cone and cylindrical shapes), dome-cylindrical (combination of hemispherical and cylindrical shapes), and hetro-conical (Figure 2).

3 Numerical analysis and validation of the model used

The CFD Software Package, Fluent 6.3.26, was employed in the 3D simulation of the cavity. In reality, the open cavity is surrounded by an infinite atmosphere. To model this condition in the numerical work, the flow domain is established such that the cavity is placed centrally in the large cylindrical enclosure having diameter and length about 15 times the cavity diameter. This is to ensure that the air flow within the cavity is unaffected. An isothermal boundary condition was applied to the inner wall whereas the outer wall of the cavity was assumed to be adiabatic. The atmospheric condition is applied to the outer domain. The flow and heat transfer simulation is based on the simultaneous solution of the system of equations describing the conservation of mass, momentum, and energy. These can be expressed as follows (Jiji [3]):

(i) continuity equation

$$\Delta \vec{V} = 0,$$

(ii) momentum equation

$$\rho \frac{D\vec{V}}{Dt} = \rho \{ \vec{g} - \nabla \vec{p} - \mu \nabla^2 \vec{V} \},$$

(iii) energy equation

$$\rho c_p \frac{DT}{Dt} = k \nabla^2 T.$$

The semi-implicit pressure linked equation (SIMPLE) scheme of the Fluent software is used. The convergence criteria for the residuals of continuity and the velocity equations are of the order of 10^{-3} and for the energy equation 10^{-6} . The 3D cavity model is analyzed for different inclinations by adjusting the gravity vector accordingly. Monitoring surface integrals are used to check for both iteration convergence and grid independence. The area-weighted average surface heat transfer coefficient is used to monitor for convergence [1].

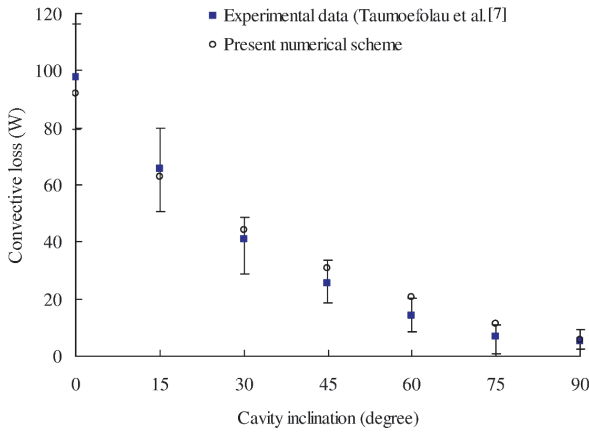


Figure 3: Validation of the present numerical scheme.

For each cavity, three-dimensional model was created using Gambit tool of CFD software package “Fluent 6.3.26”. In order to validate the numerical scheme, calculations have been carried out for convective heat loss of a cylindrical open cavity. The cavity walls are considered to be at a constant temperature. The results of calculations are compared with the experimental measurements reported by Taumoefolau et al. [7] as shown in Figure 3. It can be seen that the numerical results agree reasonably well with the experimental data. Hence the present numerical scheme is used for estimation of convective heat loss.

4 Results

In the present study, isothermal wall temperature of 723 K is used for the analysis. Temperature profile of air inside the cavity walls is shown in Figure 4 for different tilt angles for case I and case III types of cavities. As the cavity inclination increases from 0° to 90°, the volume of stagnant air increases, with the maximum being at 90°. This is observed for both categories of cavities (with and without mouth blockage). The volume of stagnation zone in case I is higher than in case III for all tilt angles and all shapes under study. Thus convective loss is expected to be less in case I type of cavities. It is also observed that the volume of the convective zone is different for each shape of the cavity. Thus convective losses are expected to vary from one shape to another. A similar behavior is seen in case II types except that the volumes of stagnant and convective zone are much bigger than in the other two cases because of increased cavity dimensions; hence convective loss is expected to be higher.

To provide quantitative support to these observations, convective zone area (A_{cb}') is calculated. It is defined as the sum of the internal wall area of the cavity below the stagnation boundary (A_{cw}) and the area of zone boundary (A_{bz}) separating stagnation and convective zone. This does not include the area of annular ring at the mouth of the aperture. There is a likelihood of presence of stagnant air

at the edge defined by the wall of the cavity and the ring. Thus, due to the presence of the ring at the aperture, air movement is constrained preventing a certain area around the edge from participating in the convection loss. In this paper, only annular ring area is excluded.

The values of A_{cb}' are calculated for all cases at each cavity inclination. These are plotted against cavity inclination in Figures 5(a), 5(c), 5(e), 5(g), and 5(i), respectively, for cavity shape cylindrical, conical, cone-cylindrical, dome-cylindrical, and hetro-conical. It shows that the value of convective zone area reduces with cavity inclination. Among the three cases under study, A_{cb}' is the lowest for case I type of cavities and the highest for case II type of cavities. To ascertain the convective loss dependency on convective zone area, Q_{conv} is plotted against cavity inclination in Figures 5(b), 5(d), 5(f), 5(h), and 5(j), respectively, for cavity shapes of cylindrical, conical, cone-cylindrical, dome-cylindrical, and hetro-conical. It is observed that the variation of Q_{conv} with cavity inclination is similar to that of variation of A_{cb}' with inclination. The trend of reduction in the convective zone area with inclination and consequently the decrease of convective loss are observed for all shapes of the cavities. Convective losses from case I type of cavities are the lowest because of their lower values of A_{cb}' among three cases as discussed earlier. Similarly, case II type of cavities exhibits more convective heat loss because of higher values of A_{cb}' .

Among the three cases, conical cavity yields the lowest convective loss whereas hetro-conical cavity gives the highest convective loss (Figures 5(d) and 5(j)). This is due to the fact that under the constraint of the same dimensional parameters (the same value of D_{ap} , D_{cav} , and L_{cav}) of different shapes, conical shape and hetro-conical shape result in, respectively, the lowest and the highest values of A_{cb}' for all tilt angles.

Radiative loss (Q_{rad}) has also been calculated for all types of cavities. It is found to be independent of cavity inclination. It is nearly constant (about 2916 W) for all shapes of the cavities of case II whereas for case III type of cavities it is about 2948 W. The configuration of cavity (with and without mouth blockage) has a less influence on radiative loss (less than 2%) for cavities with equal aperture area. This is valid for cavities operating isothermally and having the same value of emissivity for all surfaces of the cavity and aperture area. For case I type of cavities, aperture area is 36% less than other cases. Consequently, radiative loss is found to be reduced by about 36% as expected. However, investigations on decrease in heat loss of mouth-blocked cavities needed to be coupled with the estimation of concentrated flux.

5 Conclusions

Numerical three-dimensional studies of the natural convection and radiative heat loss have been investigated in

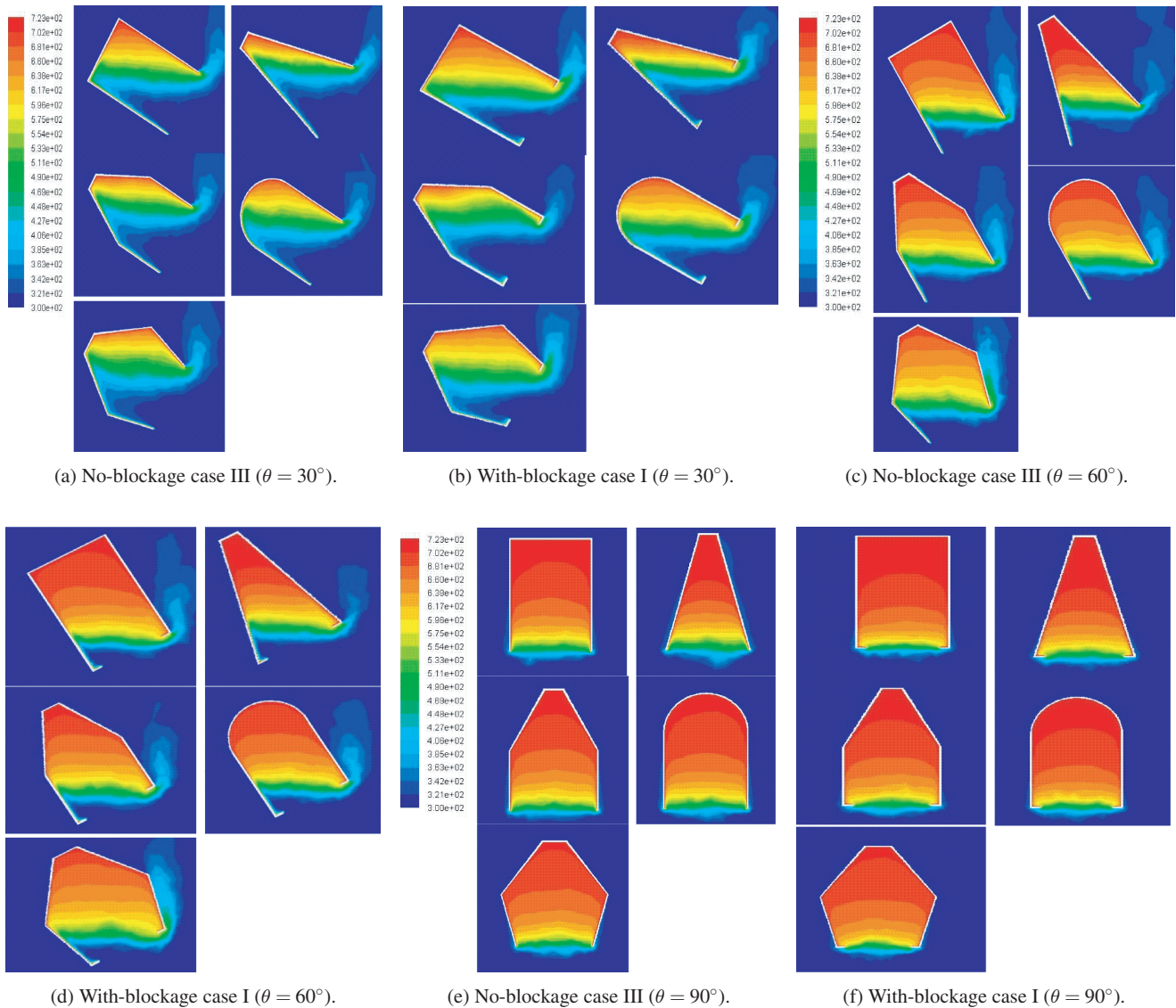


Figure 4: Temperature contours of case I and case III.

different cavities with and without mouth blockage for different tilt angles.

The following conclusions can be drawn from this study.

- (i) Convective loss decreases for cavities with mouth blockage created by reducing aperture area (case I) whereas it increases when mouth blockages are introduced by increasing cavity dimensions and keeping the same aperture area (case II).
- (ii) Convective loss is characterized by using the convective zone area. It is found to be valid for both types of cavities (with and without mouth blockage).
- (iii) Among the three cases, conical cavity yields the lowest convective loss whereas hetro-conical cavity gives the highest convective loss.
- (iv) Radiative loss is independent of cavity inclination and found to be nearly constant for all cavity shapes and cavity configurations (with or without mouth blockage) with the same aperture area. This is valid under isothermal wall condition and the same value of emissivity for each surface of the cavity. The reduction in radiative heat loss is proportional to the decrease of cavity aperture area. It is reduced by 36% in case I when the aperture area is 36% lower than the aperture area used in case II and case III.
- (v) Investigations on decrease in heat losses with mouth-blocked cavities (case I) need to be coupled with estimation of reduced values of concentrated flux input from dish reflector to identify the cavity with minimum heat loss.

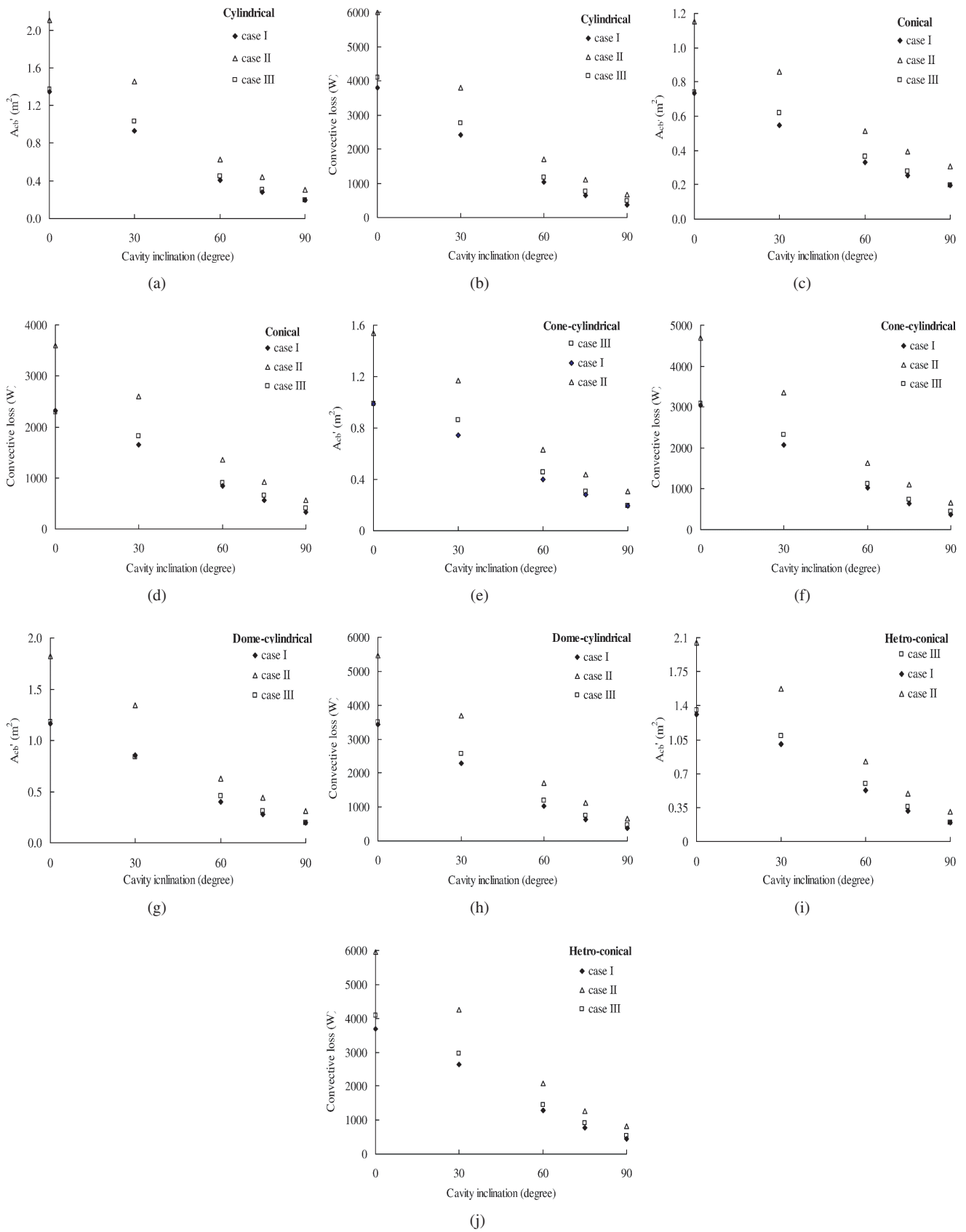


Figure 5: Variation of convective zone area and convective loss with cavity inclinations.

Nomenclature

A_{ap}	cavity aperture area [m ²]
A_{bz}	area of separation zone boundary [m ²]
A_{cb}'	convective zone area ($A_{cw} + A_{bz}$) [m ²]
A_{cw}	cavity active convective wall area [m ²]
A_w	internal cavity surface area [m ²]
D_{ap}	cavity aperture diameter [m]
D_{cav}	cavity diameter [m]
L_{cav}	cavity height [m]
Q_{conv}	convective loss [W]
Q_{rad}	radiative loss [W]
θ	cavity inclination [degree]

References

- [1] Fluent 6.3 user guide, 2006.
- [2] J. A. Harris and T. G. Lenz, *Thermal performance of solar concentrator/cavity receiver systems*, Solar Energy, 34 (1985), 135–142.
- [3] L. M. Jiji, *Heat Convection*, Springer-Verlag, Berlin, 2006.
- [4] U. Leibfried and J. Ortjohann, *Convective heat loss from upward and downward-facing cavity solar receivers: measurements and calculations*, Journal of Solar Energy Engineering, 117 (1995), 75–84.
- [5] C. G. McDonald, *Heat loss from an open cavity*, Tech. Report SAND95-2939, Sandia National Laboratories, Albuquerque, NM, 1995.
- [6] K. S. Reddy and N. Sendhil Kumar, *An improved model for natural convection heat loss from modified cavity receiver of solar dish concentrator*, Solar Energy, 83 (2009), 1884–1892.
- [7] T. Taumoefolau, S. Paitoonsurikarn, G. Hughes, and K. Lovegrove, *Experimental investigation of natural convection heat loss from a model solar concentrator cavity receiver*, Journal of Solar Energy Engineering, 126 (2004), 801–807.